ACS Catalysis

RESEARCH ARTICLE

pubs.acs.org/acscatalysis

Hybrid Sulfonic Acid Catalysts Based on Silica-Supported Poly (Styrene Sulfonic Acid) Brush Materials and Their Application in Ester Hydrolysis

Wei Long[†] and Christopher W. Jones[*,†,‡]

[†]School of Chemistry & Biochemistry and [‡]School of Chemical & Biomolecular Engineering, Georgia Institute of Technology, 311 Ferst Drive, Atlanta, Georgia 30332, United States

Supporting Information

ABSTRACT: Catalytic conversions involving water as a reactant, product, or solvent are of high importance in biomass conversion into fuels and chemicals. In this context, water-tolerant solid acids are highly valued. Polymer-oxide hybrid materials based on nonporous silica-supported sulfonic acid-containing polymer brush materials are proposed here as a new class of potentially water-tolerant solid acid catalyst. Atom transfer radical polymerization (ATRP), using both (i) an established and (ii) a new ATRP initiator that is designed to improve the hydrolytic stability of the catalyst, leads to creation of poly(styrene) brushes on the surface of fumed silica. These brushes are sulfonated to produce an acid catalyst akin to an acidic Merrifield resin, but with enhanced accessibility of the active sites. The catalysts are evaluated in the hydrolysis of ethyl lactate, with the polymer brush materials having the same activity as a homogeneous catalyst, *p*-toluenesulfonic acid, and being substantially more active than an acidic polymer resin (Amberlyst 15). The heterogeneous nature of the catalyst allows for straightforward catalyst recovery and recycle. The stability of the polymer brush catalysts depends on the nature of the initiator used, with the new alkyl-based initiator, introduced here, giving enhanced stability relative to the standard, ester-containing initiator that is most commonly used in surface-initiated ATRP. The activity of the recycled polymer brush catalysts decreased slightly in each cycle because of both desulfonation and the gradual detachment of the polymer chains from the oxide support. Oxide-supported polymer brush materials are suggested to be a promising new architecture for hybrid catalyst materials.

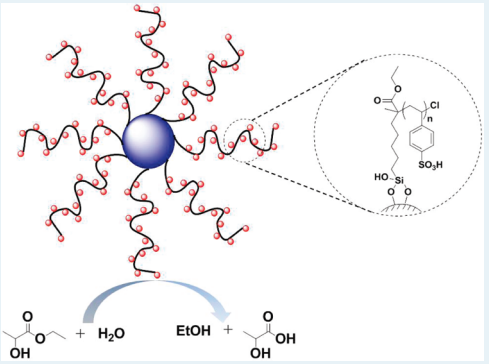

KEYWORDS: solid acid, polymer brush catalyst, biodiesel, lactic acid, aqueous stability, recycle, desulfonation

1. INTRODUCTION

Acid catalysts are extensively used in many important chemical transformations, such as alkylation and etherification.[1−3] However traditional liquid acids, such as HCl, H_2SO_4, and HF, normally cause severe equipment corrosion and environmental pollution. Solid acids, such as zeolites, oxides, phosphates, heteropoly acids, and organic−inorganic composites, have emerged as green substitutes over the last decades for liquid acids because of their easy recovery, lower pollution and lack of corrosiveness.

Generally, the catalytic activity of solid acids is negatively impacted by aqueous media, with a few exceptions, such as some organic solid acids. In many important chemical transformations, water participates as a reactant or product, such as hydrolysis and esterification reactions. For example, production of biodiesel typically involves transesterification of triglycerides with short chain alcohols and esterification of free fatty acids from feedstocks with a large amount of water.[4,5] Catalytic reactions in aqueous systems are also very attractive from the perspective of replacing organic solvents. Compared to the use of organic solvents, catalytic reactions in aqueous systems have many advantages including low cost, low toxicity and safety. Thus, it is desirable to synthesize new "water tolerant" acid catalysts and develop an understanding of acid catalyst stability in the presence of water.[6]

The two most-studied classes of organic solid acids are ion-exchange resins and inorganic oxide supported sufonic acids. Polymeric ion-exchange resins, such as the styrene-based sulfonic acids and perfluorosulfonic acid based polymer catalysts have been used commercially in many areas.[7] Sulfonic acid functionalized inorganic solids prepared via traditional postgrafting or silane co-condensation methods, such as silica supported alkyl sulfonic acids or arenesulfonic acids and Nafion/silica nanocomposites, have also been studied extensively.[8] Recently, surface initiated controlled polymerization has emerged as a new technique for material functionalization, endowing oxide surfaces with polymeric organic species. For example, surface initiated atom transfer radical polymerization (ATRP) is one of the most

Special Issue: Victor S. Y. Lin Memorial Issue

Received: February 28, 2011
Revised: May 4, 2011
Published: May 06, 2011

Scheme 1. Silica-Supported Poly(Styrene Sulfonic Acid) Brush Materials

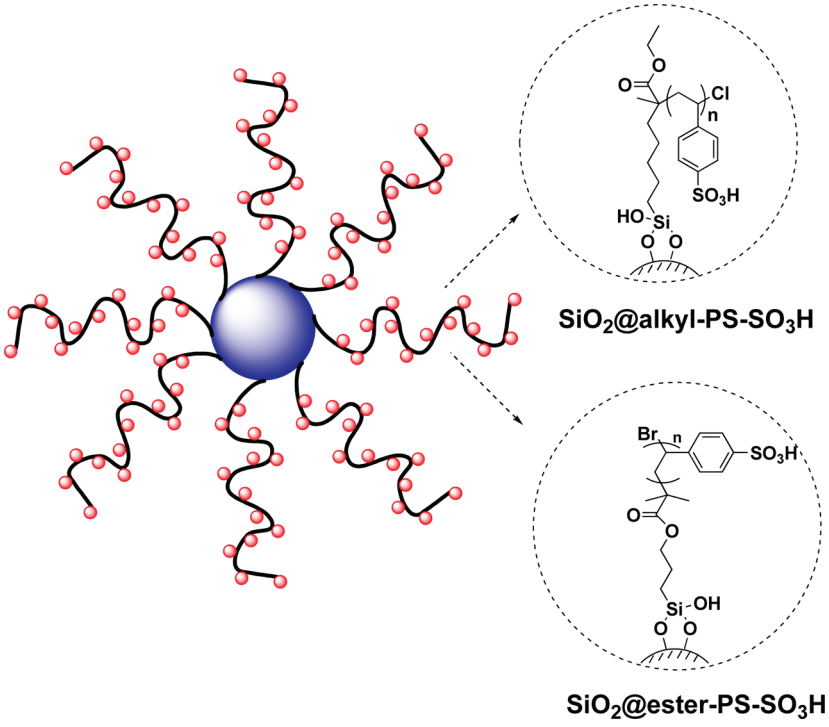

powerful and commonly used techniques to introduce uniform polymer layers on solid surfaces.[9,10] After immobilizing initiators onto the surface, the polymer chains are grown from the initiation position to form "polymer brush" materials, first described as catalysts in 2008,[11,12] that can be used to achieve high catalyst loadings while allowing good accessibility to the active sites.[11−17] In the recent literature, grafting of poly (sodium styrene sulfonate) onto SBA-15[18] and ultra large pore SBA-15[19] via ATRP of sodium styrene sulfonate has been investigated. However in those two cases, low organic loadings and acidities were achieved. A poly(vinylsulfonic acid)-grafted poly(styrene) resin has also been prepared via surface initiated radical polymerization of vinylsulfonic acid and used for catalytic esterification reactions.[20,21]

Herein, a new polymer brush supported sulfonic acid is prepared via surface initiated ATRP of styrene followed by sulfonation of the polymer brush. Cab-O-Sil M5, a nonporous silica, is used as the support to avoid potential pore clogging issues associated with polymerization with porous materials as the supports.[22,23] For typical ATRP surface initiators, there is an ester or amide linkage between the surface and the initiation site that may be hydrolytically unstable under acidic or basic conditions. To alleviate this problem, an alkyl initiator with only carbon−carbon bonds between the surface and the grafted polymer is designed and synthesized (Scheme 1). Hydrolysis of ethyl lactate is chosen as a model reaction to evaluate the activity and stability of the new acid catalyst. The product, lactic acid, is a very useful renewable chemical intermediate.[24] Lactic acid derived from fermentation processes requires extensive purification. Instead of the conventional sequential approach of reaction and separation,[25] catalytic distillation, whereby a water-tolerant acid catalyst is employed,[26−28] can be applied as a more efficient technique. In this work, new polymer brush supported sulfonic acid catalysts are used for the hydrolysis of ethyl lactate, with an emphasis placed on understanding the catalytic performance and stability of this new type of catalyst in the presence of excess water.

2. EXPERIMENTAL SECTION

2.1. Chemicals and Materials. The following chemicals were commercially available and used as received unless otherwise noted: ethyl 2-chloropropionate (Alfa Aesar, 96%), 5-bromo-1-pentene (Alfa Aesar, 96%), lithium diisopropylamide (LDA, 2 M in THF/heptane/ethylbenzene, Aldrich), tetrahydrofuran (THF, dried by passing through columns of activated copper oxide and alumina), toluene (J.T. Baker, anhydrous), dodecane (anhydrous, Sigma-Aldrich), hexamethylphosphoramide (HMPA, Aldrich, 99%), trimethoxysilane (Aldrich, 95%), Platinum(0)-1,3-divinyl-1,1,3,3,-tetramethyldisiloxane complex solution (Karstedt's catalyst, Aldrich, 0.1 M in poly(dimethylsiloxane) vinyl terminated), 1,1,4,7,10,10-hexamethyltriethylenetetramine (HMTETA, Sigma-Aldrich, 97%), (3-trimethoxysilyl) propyl 2-bromo-2-methyl propionate (Gelest, 95%), fuming sulfuric acid (Mallinckrodt, 20% SO_3), copper(I) bromide (purified by stirring in glacial acetic acid, washed with ethanol and diethyl ether, dried under vacuum and stored inside glovebox), Cab-O-Sil M5 fumed silica (Cabot Corporation, Brunauer−Emmett−Teller (BET) surface area ∼200 m^2/g), and styrene (dried over CaH_2, and purified by vacuum distillation). All air and moisture sensitive compounds were handled via Schlenk techniques or in a nitrogen glovebox.

2.2. Syntheses of New Silane-Functionalized ATRP Initiator. *Ethyl 2-Chloro-2-methyl-6-heptenoate (**1a**).* A flask containing dry THF was cooled to −78 °C, and LDA (48 mL, 96 mmol) was added into the solvent. Ethyl 2-chloro propionate (10.2 mL, 80 mmol) was then added dropwise. The reaction solution was

dx.doi.org/10.1021/cs2001175 |ACS Catal. 2011, 1, 674–681

stirred for several minutes, and then HMPA (27.9 mL, 160 mmol) was injected quickly. The color of the solution changed from deep red to dark brown. Next, 5-bromo-1-pentene (9.5 mL, 80 mmol) was added slowly to the flask. The temperature was subsequently maintained at −78 °C for 1 h with stirring. Then the mixture was allowed to warm naturally to room temperature and stirred overnight. The next day, the reaction was quenched with 25 mL of 5% HCl and 25 mL of DI H_2O. A 100 mL portion of diethyl ether was added into the mixture for extraction. The organic layer was washed with 5% HCl (5 times) and brine (2 times), and then dried over $MgSO_4$. Finally, solvents were evaporated via rotary evaporation, and the crude oil was purified by flash chromatography (95:5 hexane-EtOAc) to give 11.5 g of product (yield: 70%). ^{1}H NMR (400 MHz, $CDCl_3$): δ 1.29 (t, 3H), 1.48 (m, 2H), 1.72 (s, 3H), 2.0 (m, 4H), 4.21 (q, 2H), 5.0 (m, 2H), 5.77 (m, 1H). ^{13}C NMR (400 MHz, $CDCl_3$): δ 14.14, 24.25, 27.82, 33.48, 41.59, 62.17, 69.10, 115.25, 137.98, 171.41. (^{1}H NMR and ^{13} C NMR spectra are contained in the Supporting Information)

*Ethyl 2-Chloro-2-methyl-7-(trimethoxysilyl) Heptanoate (**1b**).* Ethyl 2-chloro-2-methyl-6-heptenoate (4.0 g, 19.5 mmol) and trimethoxysilane (3.58 g, 29.3 mmol) were added into the reaction vessel. Karstedt's catalyst (390 ul) was added into the mixture dropwise. The solution was stirred at 80 °C overnight. The crude mixture was purified with fractional vacuum distillation to give 3.2 g product (yield: 50%). ^{1}H NMR (400 MHz, $CDCl_3$): δ 0.63 (m, 2H), 1.30 (t, 3H), 1.37 (m, 6H), 1.72 (s, 3H), 1.98 (m, 2H), 3.57 (s, 9H), 4.22 (q, 2H). ^{13}C NMR (400 MHz, $CDCl_3$): δ 9.12, 14.10, 22.47, 24.62, 27.71, 32.86, 42.05, 50.56, 62.99, 69.18, 171.44. (^{1}H NMR and ^{13} C NMR spectra are contained in the Supporting Information)

Silica Supported ATRP Initiators. Cab-O-Sil M5 (2 g) was dispersed into toluene (86 g) with sonication in a 150 mL pressure tube.

Ethyl 2-chloro-2-methyl-7-(trimethoxysilyl) heptanoate (4 mmol) was added slowly into the slurry and then the mixture was refluxed about 40 h. The solid was recovered by filtration through filter paper and washed repeatedly with toluene, petroleum ether, methanol, and diethyl ether. The recovered white powder was dried under vacuum at 100 °C for several hours and then stored in a glovebox for later use. Thermal gravimetric analysis (TGA) revealed that the organic loading of the supported chloro heptanoate (SiO_2@alkyl initiator) was 0.53 mmol/g.

(3-Trimethoxysilyl) propyl 2-bromo-2-methyl propionate was immobilized to the silica surface with the same procedure. The organic loading of the supported bromo isobutyrate (SiO_2@ester initiator) was 0.23 mmol/g by TGA, which is lower than that of the SiO_2@alkyl initiator. The syntheses of SiO_2@alkyl initiator and SiO_2@ester initiator were repeated several times, and the resulting loadings were consistent.

To obtain a SiO_2@ester initiator with higher initiator loading, the ratio of initiator silane to Cab-O-Sil was increased from 2 mmol silane/g SiO_2 to 5 mmol silane/g SiO_2. The organic loading of SiO_2@ester initiator_2 was 0.44 mmol/g, as determined via TGA.

2.3. Preparation of Catalysts. *Surface-Initiated ATRP.* The surface-initiated ATRP was performed according to reported procedures[11] with minor modifications. Silica supported initiator (SiO_2@alkyl initiator, 899 mg) was suspended into anhydrous toluene (19.4 g) to give a slurry of 40 mg/mL. The molar ratios of reactants were as follows: styrene/SiO_2@alkyl initiator/CuBr/HMTETA = 50:1:1.2:2.4. The mixture was stirred under nitrogen at 110 °C for 24 h. A small amount of dodecane was added as the standard to monitor the conversion of the polymerization. At the end, the polymerization solution was diluted with excess toluene, and the solid product was recovered by centrifuge (8000 rpm, 30 min). This step was repeated at least three times to wash away the free polymer (if any formed) during the polymerization. Then the solid was washed repeatedly with a mixture of methanol and pyridine to remove the copper catalyst residue. The final recovered powder sample was dried under vacuum at 100 °C for several hours. For the SiO_2@ester initiator, all the experimental parameters and the synthesis procedure were the same except a higher ratio of styrene to SiO_2@ester initiator was used (80:1). For SiO_2@ester initiator_2, all the experimental parameters and the synthesis procedures were the same.

Synthesis of Polymer Brush Supported Sulfonic Acids. The polymer brush materials were sulfonated following a published literature[29] with slight modifications. In a typical sulfonation, the polymer brush material (1 g) was added into a 50 mL flask. Fuming sulfuric acid (25 mL, 48 g) was weighed in a small vial and then transferred into the flask. The slurry was shaken for 10 min, and then was quenched by slowly adding the mixture into excess DI H_2O. The recovered acid catalyst was washed repeatedly with DI H_2O until the pH of the filtrate was above 6. The catalyst was dried under vacuum at 100 °C overnight.

2.4. Characterization. ^{1}H and ^{13}C NMR spectra were acquired with a Varian Mercury Vx 400 ($CDCl_3$ solvent). Transmission electron microscopy (TEM) measurements were performed on a JEOL 100CX-2 and HF 2000. A Netzsch STA 409 was used for TGA under a mixture of air and nitrogen with a heating rate of 10 °C/min. FT-IR spectra were obtained on a Bruker Vertex 80 optical bench using KBr Pellets. Surface areas were assessed via nitrogen physisorption analysis using a Micromeritics TristarII. Before measurement, the samples were degassed overnight under vacuum around 100 °C. X-ray Photoelectron Spectroscopy (XPS) was performed on a Thermo K-Alpha XPS using Al Kα irradiation with a flood gun. The samples were put on a powder sample holder, evacuated in a load lock, and then transferred to the analysis chamber (vacuum around E-08 mbar) for measurement. The spectra were referenced to the C1s peak at 284.8 eV. The reaction conversion was monitored by gas phase chromatography (GC) on a Shimadzu GC-2010 with a FID detector and a SHRX5 column. Elemental analyses were performed by Columbia Analytical Services (Tucson, AZ). Titration was used to determine the acid loading of the catalysts. The polymer brush supported sulfonic acid (∼ 15 mg) was dispersed into a saturated NaCl aqueous solution (∼ 5 mL) for several hours under sonication. The solid was filtered and washed several times with brine. The collected filtrate (∼20 mL) was titrated with 0.01 M NaOH with phenolphthalein as the indicator.

2.5. Catalytic Hydrolysis of Ethyl Lactate. Typically, the catalyst (SiO_2@alkyl-PS-SO_3H, 48 mg, 1.25 mol % catalyst relative to the ethyl lactate, equivalent to 0.144 mmol H^+) was weighed into a 15 mL two-neck flask and was dispersed into 1 g of DI H_2O via sonication (∼ 30 min). 1,4-Dioxane (1.03 g, internal standard) was added to the dispersed catalyst. The reaction flask with a condenser was immersed into an oil bath and preheated to 60 °C (∼20 min). Ethyl lactate (1.37 g, 11.6 mmol) and DI H_2O (2.14 g) were mixed together and transferred into the two-neck flask to start the reaction. Samples (40 ul) were removed periodically via syringe and analyzed by GC-FID. The hydrolysis of ethyl lactate with SiO_2@ester-PS-SO_3H was performed following the same procedures. In all the reactions, 1.25 mol % of

dx.doi.org/10.1021/cs2001175 |*ACS Catal.* 2011, 1, 674–681

Scheme 2. Synthesis of Ethyl 2-Chloro-2-methyl-7-(trimethoxysilyl) Heptanoate

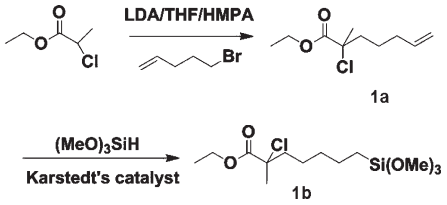

the catalyst was used, and the reactants and the standard were scaled according to the amount of catalysts used. At the end of the reaction, the catalyst was recovered by filtration and washed repeatedly with DI H_2O until the pH of the filtrate was above 6. The recovered catalysts were dried under vacuum overnight at 100 °C, and then reused in subsequent reactions. Recycle experiments were scaled according to the mass of the recovered catalysts.

3. RESULTS AND DISCUSSION

3.1. Synthesis of the ATRP Initiator Silanes. For preparation of the polymer brush materials, the synthesis was carried out in two steps: (1) immobilization of the initiator on the solid support; (2) surface initiated polymerization. The most commonly used silane-functionalized ATRP initiators all have amide or ester linkages between the silicon atom and the polymerization initiation point, and therefore they may be unstable under acidic or basic aqueous conditions. For example, several reports from Rühe et al. describe a system whereby grafted polymers were detached from the surface by cleaving the ester bond in the initiator moiety between the surface and the polymer chain under reflux conditions with *p*-toluenesulfonic acid as the catalyst.[30,31] Since our target catalyst is a polymer brush supported sulfonic acid, to achieve better catalytic stability, a new initiator was designed and synthesized (Scheme 2). In this new initiator, instead of the ester linkage, there are only C−C bonds between the surface and the initiation position. The initiator precursor was functionalized by adding a pentene group next to the initiation position. A trimethoxysilane group was then added to the olefin via hydrosilylation in the presence of Karstedt's catalyst at 80 °C. A small number of samples were taken and checked with ^{1}H NMR during the course of the hydrosilylation to monitor the reaction. The peaks corresponding to the olefin group disappeared gradually. The final product was purified via fractional vacuum distillation. The distillate at 160 °C under 30 mmtorr contained the desired product, **1b**.

3.2. Preparation of the Supported Initiator. Cab-O-Sil M5 is a fumed, nonporous silica with multiparticle aggregates. The average aggregate length is 0.2−0.3 μm, and the surface area is ~200 m^2/g. ATRP initiator species were deposited onto the silica surface by refluxing the initiator silane and silica in toluene. Unreacted silane was removed by extensive washing with toluene, petroleum ether, methanol, and diethyl ether. The organic loading of the silica supported initiator was estimated by TGA (Table 1). The immobilization of each initiator silane was performed following the same procedures and repeated multiple times. The loadings of the SiO_2@alkyl initiator were always higher than those of the SiO_2@ester initiator, which may be due to the different reactivities of these two initiator silanes. This results in slightly different initiator loadings on the surface of the silica support. The densities of the supported initiators were between 0.7−1.6/nm^2, which is lower than the silanol density of the fumed silica (2−4 OH/nm^2).[32]

Table 1. Loading and Density of the Supported Initiator

materials	mmol of initiator/ g of sample	no. of initiators/ nm^2 of surface[a]
SiO_2@alkyl initiator	0.53	1.6
SiO_2@ester initiator	0.23	0.70

[a] Calculation shown in Supporting Information.

Table 2. Physical Characteristics of the Polymer Brush Materials Prepared via Surface Initiated ATRP

materials	[M]/[SiO_2@ initiator]	conv.	$[M]_{polymerized}$/[SiO_2@ initiator]	organic loading	organic loading after rewashing
SiO_2@alkyl-PS	50	64%	32	60.2%	61.7%
SiO_2@ester-PS	80	41%	32.8	41.1%	40.7%

FT-IR and XPS were used to further confirm the surface species in the hybrid materials. In the FT-IR spectra (Supporting Information, Figure S5), the peaks around 2930 cm^{-1} were assigned to aliphatic C−H stretches, and the C═O stretch was clearly visible at 1720 cm^{-1}. XPS analysis (Supporting Information, Figure S6a) of the silica supported alkyl initiator also clearly revealed the characteristic peak of Cl 2p at 200.4 eV (for SiO_2@ester initiator, the Br 3d peak was evident at 69.6 eV).

3.3. Surface Initiated ATRP of Styrene. The silica supported initiators were used for ATRP of styrene. Typically, the initiator functionalized silica was mixed with styrene, copper(I) bromide, ligand, toluene, and internal standard at 110 °C for 24 h. The monomer conversion was determined at the end of polymerization via GC-FID. Since the initiator density and initiation efficiency of SiO_2@alkyl initiator were different from that of SiO_2@ester initiator, polymerization under identical conditions yielded significantly different polymer loadings and characteristics. To attempt to yield catalysts that had comparable polymer loadings using the two initiator-functionalized solids, the [monomer]/[initiator] ratio was tuned to yield the same ratio of the polymerized monomer to the supported initiator (= [styrene]/[SiO_2@initiator] × conversion). Although these values were similar for the two materials, the polymer content of the produced SiO_2@alkyl-PS was still higher than that of the SiO_2@ester-PS because the initiator loading of the SiO_2@alkyl initiator was higher. The recovered polymer brush materials were washed extensively with toluene to remove free polymer to mitigate its potential effects on the subsequent catalytic investigations. The organic loadings of the polymer brush materials were estimated by TGA (Table 2). According to the calculations (Supporting Information, Table S1), the majority of the polymerized styrene was growing on the surface. Although a small amount of free polymer was likely formed, it could be removed by repeated washing. To ensure that the free polymer was removed, the washing procedures were repeated, and it was found that the organic loadings of the polymer brush materials did not change. This suggests that the two catalysts, SiO_2@alkyl-PS and SiO_2@ester-PS, were devoid of free polymer and all polymers were covalently bound to the oxide surface. FT-IR confirmed that the structure of the polymer layer in the solid materials was consistent with poly(styrene) (Supporting Information, Figure S5c). Aromatic C−H stretches were observed around 3030 cm^{-1} and a significant growth of peaks associated with

dx.doi.org/10.1021/cs2001175 |ACS Catal. 2011, 1, 674–681

Scheme 3. Preparation of SiO_2@alkyl-PS-SO_3H

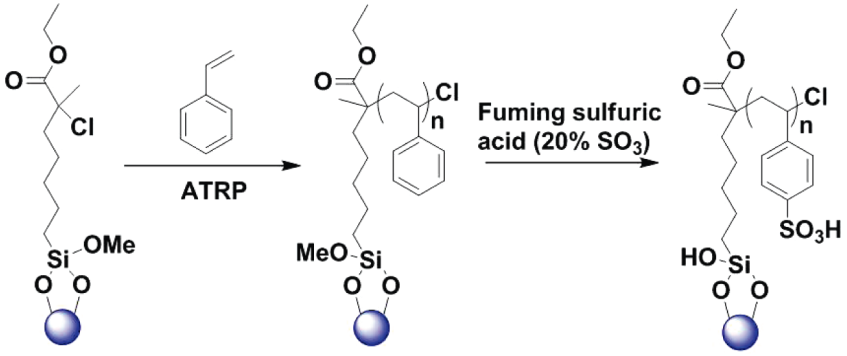

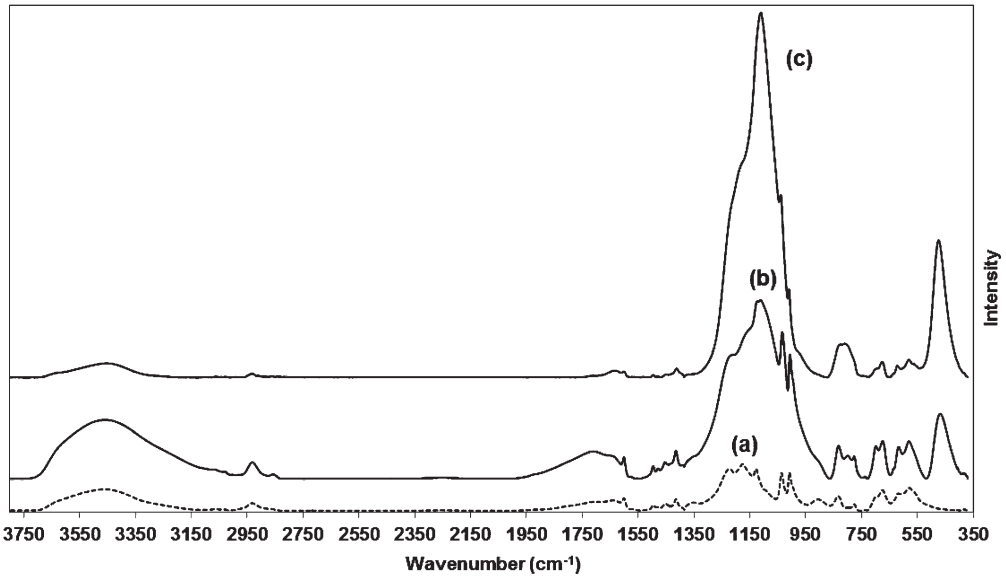

Figure 1. FT-IR of Amberlyst 15 (a); SiO_2@alkyl-PS-SO_3H (b); SiO_2@ester-PS-SO_3H (c). Amberlyst 15 is sulfonic acid resin based on cross-linked styrene-divinylbenzene copolymers.

the polymer backbone, assigned to aliphatic C−H stretches around 2930 cm^{-1}, was also observed. In the TEM images, the Cab-O-Sil supported poly(styrene) material (Supporting Information, Figure S7) displayed a fractal-like structure with a thin layer of polymer on the surface.

3.4. Sulfonation of the Poly(styrene) Brushes. After treatment with fuming sulfuric acid,[29,33] $-SO_3H$ groups were introduced into SiO_2@alkyl-PS (Scheme 3) and SiO_2@ester-PS (the catalysts are denoted as SiO_2@alkyl-PS-SO_3H and SiO_2@ester-PS-SO_3H). Since the sulfonation reactions are typically electrophilic substitutions, the $-SO_3H$ group is added to the ortho or para positions in the aromatic ring, and monosubstitution is preferred.[33] The successful sulfonation was verified by FT-IR, XPS, elemental analysis, and titration. In the FT-IR spectra (Figure 1), the S═O stretches at 1008 cm^{-1} and 1037 cm^{-1} clearly indicated the existence of sulfonic acids.[34,35] In the XPS spectra (Figure 2), the S 2p peak at 169.1 eV was observed.[29] The XPS analysis showed that the S/C ratios of SiO_2@alkyl-PS-SO_3H and SiO_2@ester-PS-SO_3H were 0.146 and 0.140, respectively. The data suggest the SiO_2@alkyl-PS-SO_3H and SiO_2@ester-PS-SO_3H have similar surface sulfonation degrees. This value is also close to 0.125, which is the theoretical value of the S/C ratio assuming each aromatic ring bears one sulfonic acid group in the poly(styrene) polymers. The results from elemental analysis (Table 3) were consistent with the information interpreted from the XPS analysis. The compiled data reveal that both of the catalysts have similar sulfonation degrees and the S/C molar ratios were close to the theoretical ones.

The ion exchange capacity of the catalysts was determined by acid−base titration.[36,37] The acid loadings of SiO_2@alkyl-PS-SO_3H and SiO_2@ester-PS-SO_3H determined by titration were 3.0 mmol/g and 1.3 mmol/g, respectively. The results were consistent with the values from elemental analysis (Table 3). For polymer brush supported sulfonic acids prepared by the new synthesis strategy utilizing the alkyl-linked initiator, a much higher acid loading could be achieved, compared to other silica supported sulfonic acids, which usually have acid loadings of less than 1 mmol/g. Furthermore, it should be noted that the carbon content of the SiO_2@alkyl-PS-SO_3H was reduced slightly from 130 mmol C/g SiO_2 to 96 mmol C/g SiO_2, after sulfonation. In contrast, the C content of the SiO_2@ester-PS-SO_3H decreased dramatically from 51 mmol C/g SiO_2 to 19 mmol C/g SiO_2 after sulfonation. This observation suggests the majority of the polymer

dx.doi.org/10.1021/cs2001175 |ACS Catal. 2011, 1, 674–681

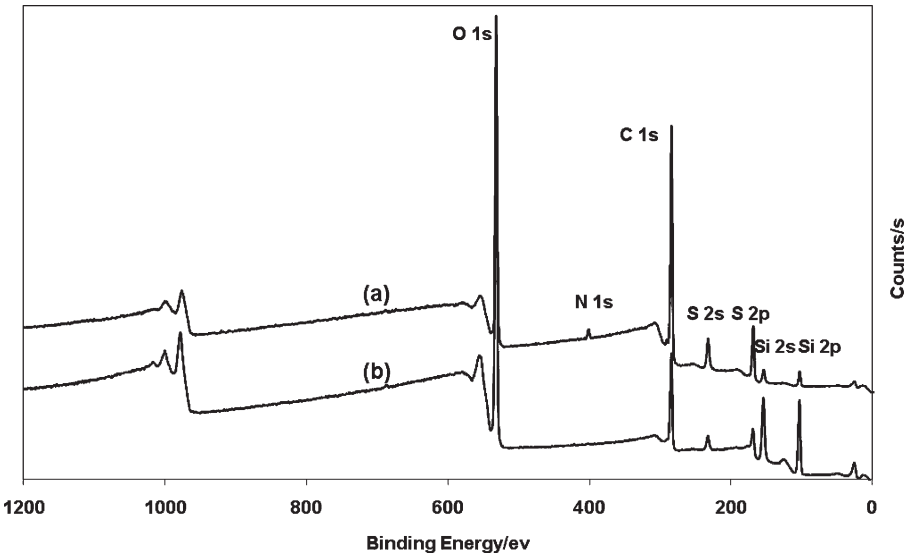

Figure 2. XPS spectra of SiO_2@alkyl-PS-SO_3H (a); SiO_2@ester-PS-SO_3H (b).

Table 3. Compositions of Solid Polymer Brush Materials after Sulfonation

catalysts	S (mmol/g)	C (mmol/g)	S/C	sulfonation degree
SiO_2@alkyl-PS-SO_3H	3.26	27.6	0.118	~94%
SiO_2@ester-PS-SO_3H	1.51	13.02	0.116	~93%

matrix remained in the SiO_2@alkyl-PS-SO_3H catalyst after sulfonation, while a large percentage of polymers detached from the silica support in SiO_2@ester-PS-SO_3H during the sulfonation process. These observations show the polymer brush sulfonic acid catalyst based on the alkyl initiator has better stability compared to the material made with the ester initiator.

The thermal stability of the catalyst was determined by TGA. For example, in SiO_2@alkyl-PS-SO_3H (Supporting Information, Figure S8), a three step decomposition pattern was observed. A slight mass loss around 100 °C was attributed to removal of water bound to the hydrophilic sulfonic acid groups. A second mass loss was observed around 310 °C, which is likely associated with desulfonation.[38] The final mass loss was likely due to decomposition of polymer matrix at around 560 °C.

3.5. Catalytic Hydrolysis of Ethyl Lactate. The catalytic activity and recyclability of the polymer brush sulfonic acid catalysts were demonstrated in the hydrolysis of ethyl lactate. The polymer brush supported sulfonic acids displayed similar activity (Figure 3) to their homogeneous analogue, *p*-toluenesulfonic acid, and a much higher reaction rate compared to Amberlyst 15, which is attributed to the easy accessibility of the active sites originating from the unique polymer brush architecture. For SiO_2@alkyl-PS-SO_3H, the catalyst showed good activity over three runs (Figure 4a), with only a slight decrease in the reaction rate upon recycle. Titration of the recovered SiO_2@alkyl-PS-SO_3H catalyst showed that the acid loading decreased from 3.0 mmol/g to 2.8 mmol/g after cycle 1 (7% loss) and then to 2.4 mmol/g after cycle 2 (20% loss). For SiO_2@ester-PS-SO_3H, the reaction rate in the first run was similar to that of the SiO_2@alkyl-PS-SO_3H (Figure 3). This suggests the two catalysts have similar accessibility of the active sites under these conditions,

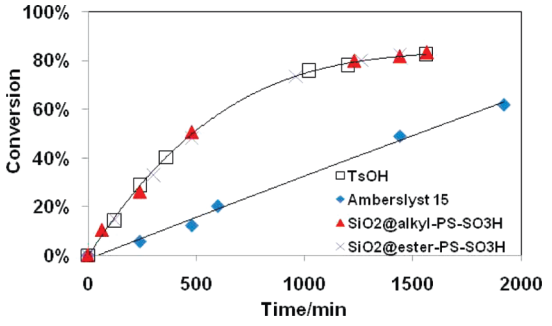

Figure 3. Kinetics of ethyl lactate hydrolysis. (1.25 mol % catalyst loading, 60 °C).

despite the different polymer surface coverage (reactions were run at the same acid loading). The SiO_2@ester-PS-SO_3H catalyst deactivated more quickly (Figure 4b), and the acid loading was reduced from1.3 mmol/g to 0.87 mmol/g after cycle 2 (33% loss).

The decrease of acid loading may be attributed to desulfonation or the detachment of the polymer chains from the surface. FT-IR (Supporting Information, Figure S9 and S10) was used to assess the functional groups of the recycled catalysts. Compared to the fresh catalysts, the recycled ones did not have significant differences in the spectra. The peaks corresponding to the S═O stretches could still be clearly observed in the spectra of the recycled catalysts. For further understanding of the deactivation mechanisms, more quantitative analysis of the composition of the catalysts was performed by elemental analysis. It was found that the S/C ratio decreased gradually in the SiO_2@alkyl-PS-SO_3H, (Supporting Information, Table S2), which indicated desulfonation[39] occurred during the ester hydrolysis reactions. The C/Si ratios also decreased slightly after recycle, which is probably due to the hydrolysis of the Si—O—Si bonds that connect the initiator group to the silica surface.[40,41] As for the SiO_2@ester-PS-SO_3H catalyst, it displayed similar trends (Supporting Information, Table S3) except the carbon content decreased more quickly (Figure 5).

Since polymer detachment was observed in both of the catalysts, to shed light on the effects of polymer coverage on the material stability, SiO_2@ester-PS_2 with a similar polymer

dx.doi.org/10.1021/cs2001175 |*ACS Catal.* 2011, 1, 674–681

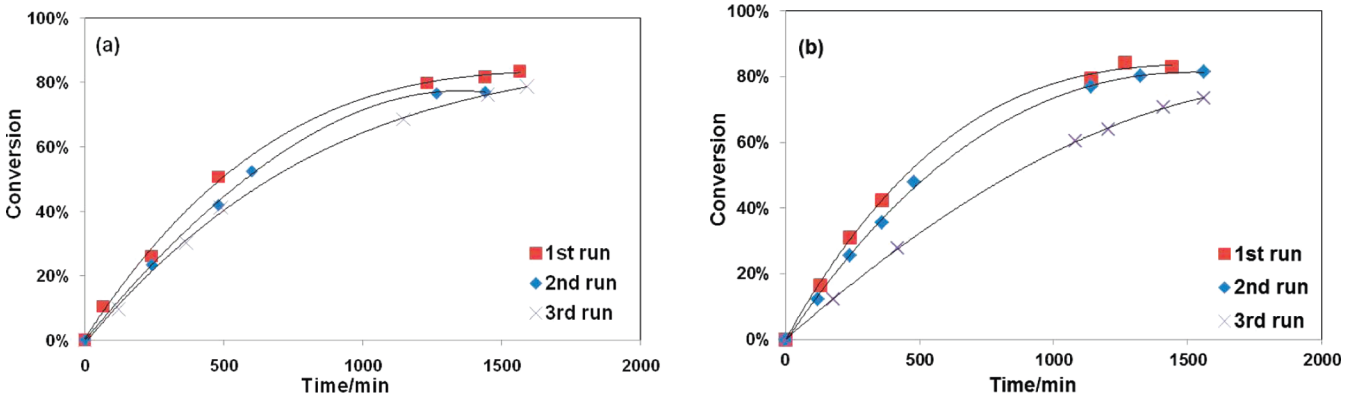

Figure 4. Kinetics of the catalysts during recycles: SiO_2@alkyl-PS-SO_3H (a); SiO_2@ester-PS-SO_3H (b). (1.25 mol % catalyst loading, 60 °C).

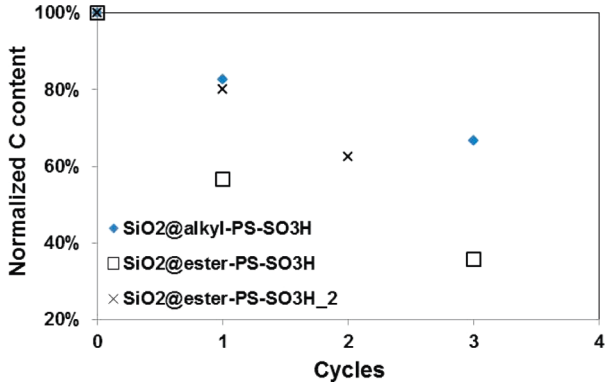

Figure 5. Normalized carbon content of the catalysts after each cycle (define the C mmol/g in the fresh catalyst as 100%).

loading (Supporting Information, Table S4) to SiO_2@alkyl-PS was prepared. After sulfonation, the C content of the SiO_2@ester-PS-SO_3H_2 decreased from 118 mmol C/g SiO_2 to 68 mmol C/g SiO_2 (43% decrease, compared to 27% decrease in SiO_2@alkyl-PS-SO_3H and 65% decrease in SiO_2@ester-PS-SO_3H). The acid loading of the fresh catalyst was 2.8 mmol/g. The activity and stability of SiO_2@ester-PS-SO_3H_2 catalyst were tested in the ethyl lactate hydrolysis test reaction. Consistently, the fresh catalyst displayed a similar reaction rate to the other two polymer brush supported sulfonic acids, but deactivated gradually during recycle, with a slightly higher deactivation rate than SiO_2@alkyl-PS-SO_3H (Supporting Information, Figure S11). The C/Si ratio (Supporting Information, Table S5) was also reduced in the reused catalysts. The trend of carbon loss (Figure 5) is faster compared to that of SiO_2@alkyl-PS-SO_3H, while slower than that of the original SiO_2@ester-PS-SO_3H. All the observations further indicated the polymer brush sulfonic acid based on the alkyl initiator had better stability compared to the material made with the ester initiator. The improved stability of SiO_2@ester-PS-SO_3H_2 compared to SiO_2@ester-PS-SO_3H is suggested to be due to the increased initiator silane coverage on the surface and higher polymer content in the material, giving a denser coverage of protecting polymer around the support.

4. CONCLUSIONS

Silica particles functionalized with poly(styrene sulfonic acid) brushes were prepared via ATRP for use as acid catalysts containing highly accessible acid sites with high loading. The polymer brush catalysts were demonstrated in the hydrolysis of ethyl lactate and shown to be equally active to a homogeneous analogue, *p*-toluenesulfonic acid, as well as substantially more active than a traditional polymer resin catalyst, Amberlyst 15. A new ATRP initiator designed to be more hydrolytically stable was prepared, and the resulting polymer brush catalyst, SiO_2@alkyl-PS-SO_3H, was shown to have improved stability relative to the catalysts made with a traditional ATRP initiator containing an ester group, SiO_2@ester-PS-SO_3H. Nonetheless, the catalysts deactivated slightly over several uses because of polymer loss and desulfonation. The polymer brush architecture is suggested to be a useful approach to preparation of polymeric catalysts with a high loading of accessible active sites and the architecture merits further development.

■ ASSOCIATED CONTENT

Supporting Information. ^1H and ^{13}C NMR of ethyl 2-chloro-2-methyl-6-heptenoate and ethyl 2-chloro-2-methyl-7-(trimethoxysilyl) heptanoate; FT-IR, XPS, TGA, TEM, and elemental analysis of materials and catalysts. This material is available free of charge via the Internet at http://pubs.acs.org.

■ AUTHOR INFORMATION

Corresponding Author

*E-mail: cjones@chbe.gatech.edu.

Funding Sources

This work was partially supported by the U.S. Department of Energy, Basic Energy Sciences, for financial support through Catalysis Science Grant/Contract No. DE-FG02-03ER15459. The work was also partially supported by the U.S. National Science Foundation (Grant CBET-055354). C.W.J. thanks the School of Chemical & Biomolecular Engineering at Georgia Tech for support via the J. Carl & Sheila Pirkle Fellowship.

■ ACKNOWLEDGMENT

C.W.J. acknowledges the outstanding work of Prof. Victor S. Y. Lin of Iowa State University as inspiration for our work on organic−inorganic hybrid catalysts. This work is dedicated to his memory.

REFERENCES

(1) Corma, A. *Chem. Rev.* **1995**, *95*, 559–614.
(2) Busca, G. *Chem. Rev.* **2007**, *107*, 5366–5410.
(3) Wong, W.-L.; Ho, K.-P.; Lee, L. Y. S.; Lam, K.-M.; Zhou, Z.-Y.; Chan, T. H.; Wong, K.-Y. *ACS Catal.* **2011**, *1*, 116–119.
(4) Melero, J. A.; Iglesias, J.; Morales, G. *Green. Chem.* **2009**, *11*, 1285–1308.
(5) Fang, D. Y., J.; Jiao, C. *ACS Catal.* **2011**, *1*, 42–47.
(6) Okuhara, T. *Chem. Rev.* **2002**, *102*, 3641–3665.
(7) Harmer, M. A.; Sun, Q. *Appl. Catal., A* **2001**, *221*, 45–62.
(8) Melero, J. A.; van Grieken, R.; Morales, G. *Chem. Rev.* **2006**, *106*, 3790–3812.
(9) Barbey, R.; Lavanant, L.; Paripovic, D.; Schuwer, N.; Sugnaux, C.; Tugulu, S.; Klok, H. A. *Chem. Rev.* **2009**, *109*, 5437–5527.
(10) Zhao, B.; Zhu, L. *Macromolecules* **2009**, *42*, 9369–9383.
(11) Gill, C. S.; Venkatasubbaiah, K.; Phan, N. T. S.; Weck, M.; Jones, C. W. *Chem.—Eur. J.* **2008**, *14*, 7306–7313.
(12) Zhao, B.; Jiang, X. M.; Li, D. J.; Jiang, X. G.; O'Lenick, T. G.; Li, B.; Li, C. Y. *J. Polym. Sci., Part A: Polym. Chem.* **2008**, *46*, 3438–3446.
(13) Jiang, X. M.; Wang, B. B.; Li, C. Y.; Zhao, B. *J. Polym. Sci., Part A: Polym. Chem.* **2009**, *47*, 2853–2870.
(14) Gill, C. S.; Long, W.; Jones, C. W. *Catal. Lett.* **2009**, *131*, 425–431.
(15) Costantini, F.; Bula, W. P.; Salvio, R.; Huskens, J.; Gardeniers, H.; Reinhoudt, D. N.; Verboom, W. *J. Am. Chem. Soc.* **2009**, *131*, 1650–+.
(16) Costantini, F.; Benetti, E. M.; Tiggelaar, R. M.; Gardeniers, H.; Reinhoudt, D. N.; Huskens, J.; Vancso, G. J.; Verboom, W. *Chem.—Eur. J.* **2010**, *16*, 12406–12411.
(17) O'Lenick, T. G.; Jiang, X. M.; Zhao, B. *Polymer* **2009**, *50*, 4363–4371.
(18) Li, C. M.; Yang, J.; Wang, P. Y.; Liu, J.; Yang, Q. H. *Microporous Mesoporous Mater.* **2009**, *123*, 228–233.
(19) Martin, A.; Morales, G.; Martinez, F.; van Grieken, R.; Cao, L.; Kruk, M. *J. Mater. Chem.* **2010**, *20*, 8026–8035.
(20) Okayasu, T.; Saito, K.; Nishide, H.; Hearn, M. T. W. *Chem. Commun.* **2009**, 4708–4710.
(21) Okayasu, T.; Saito, K.; Nishide, H.; Hearn, M. T. W. *Green. Chem.* **2010**, *12*, 1981–1989.
(22) Drese, J. H.; Choi, S.; Lively, R. P.; Koros, W. J.; Fauth, D. J.; Gray, M. L.; Jones, C. W. *Adv. Funct. Mater.* **2009**, *19*, 3821–3832.
(23) Wilson, B. C.; Jones, C. W. *Macromolecules* **2004**, *37*, 9709–9714.
(24) Zhang, J. Z., Y.; Pan, M.; Feng, X.; Ji, W.; Au, C. T. *ACS Catal.* **2011**, *1*, 32–41.
(25) Sun, X. W., Q.; Zhao, W.; Ma, H.; Sakata, K. *Sep. Purif. Technol.* **2006**, *49*, 43–48.
(26) Sanz, M. T.; Murga, R.; Beltran, S.; Cabezas, J. L.; Coca, J. *Ind. Eng. Chem. Res.* **2002**, *41*, 512–517.
(27) Sanz, M. T.; Murga, R.; Beltran, S.; Cabezas, J. L.; Coca, J. *Ind. Eng. Chem. Res.* **2004**, *43*, 2049–2053.
(28) Delgado, P.; Sanz, M. T.; Beltran, S. *Chem. Eng. J.* **2007**, *126*, 111–118.
(29) Feyen, M.; Weidenthaler, C.; Schuth, F.; Lu, A. H. *Chem. Mater.* **2010**, *22*, 2955–2961.
(30) Prucker, O.; Ruhe, J. *Macromolecules* **1998**, *31*, 592–601.
(31) Rühe, J. K., W. *Polym. Rev.* **2002**, *42*, 91–138.
(32) Hubbard, A. T. *Encyclopedia of Surface and Colloid Science: Por-Z*; Marcel Dekker, Inc.: New York, 2002; Vol. 4.
(33) Kučera, F. J., J. *Polym. Eng. Sci.* **1998**, *38*, 783–792.
(34) Xing, R.; Liu, N.; Liu, Y. M.; Wu, H. W.; Jiang, Y. W.; Chen, L.; He, M. Y.; Wu, P. *Adv. Funct. Mater.* **2007**, *17*, 2455–2461.
(35) Liu, F. J.; Meng, X. J.; Zhang, Y. L.; Ren, L. M.; Nawaz, F.; Xiao, F. S. *J. Catal.* **2010**, *271*, 52–58.
(36) Jones, C. W.; Tsuji, K.; Davis, M. E. *Nature* **1998**, *393*, 52–54.
(37) Gill, C. S.; Price, B. A.; Jones, C. W. *J. Catal.* **2007**, *251*, 145–152.
(38) Nasef, M. M.; Saidi, H.; Nor, H. M. *J. Appl. Polym. Sci.* **2000**, *77*, 1877–1885.
(39) Melero, J. A.; Stucky, G. D.; van Grieken, R.; Morales, G. *J. Mater. Chem.* **2002**, *12*, 1664–1670.
(40) Yang, H. Q.; Zhang, G. Y.; Hong, X. L.; Zhu, Y. Y. *Microporous Mesoporous Mater.* **2004**, *68*, 119–125.
(41) Riachi, C.; Schuwer, N.; Klok, H. A. *Macromolecules* **2009**, *42*, 8076–8081.